Proceedings of the 9th U.S. National and 10th Canadian Conference on Earthquake Engineering
Compte Rendu de la 9ième Conférence Nationale Américaine et
10ième Conférence Canadienne de Génie Parasismique
July 25-29, 2010, Toronto, Ontario, Canada • Paper No

COMPARATIVE SEISMIC RESPONSE OF CODE DESIGNED CONVENTIONAL AND BASE-ISOLATED BUILDINGS TO SCENARIO EVENTS

K. L. Ryan[1], E. Erduran[2], P. J. Sayani[3], N. D. Dhao[4]

ABSTRACT

In this study, the seismic response of code-designed conventional and base-isolated steel moment frame and braced frame buildings is evaluated. Three dimensional models for both buildings are created and seismic response is assessed for three scenario earthquakes. The response history analysis results indicate that the performance of the isolated building is superior to the conventional building in the design event. However, yielding is observed in the MCE, and statistical outliers, especially in the moment frame, reduce confidence that the isolated building provides superior performance to its conventional counterpart. The outliers observed in the response of isolated buildings are disconcerting and need careful evaluation in future studies.

Introduction

The principal benefit of seismic isolation for buildings, to offer far superior performance in a design level earthquake, is generally accepted and recognized by structural engineers. Flexible devices installed at the base that lengthen the natural period allow an isolated building to accommodate the reduced design forces elastically, eliminating structural damage and greatly reducing the damage in acceleration-sensitive nonstructural components. However, the seismic performance objectives are only implicitly embedded in U.S. code design standards (e.g. ASCE, 2005), and the performance benefits of seismic isolation generally are not recognized by building owners and decision makers. Even sophisticated owners that require higher performance are constrained by initial costs, and often opt for alternative systems when faced with additional complexities of seismic isolation. Seismic isolation has the potential to be more routinely adopted if reliable analysis tools are available to predict economic outcomes.

The overarching objective of our study is to comparatively evaluate the life cycle performance of code-designed steel buildings using the PEER loss estimation methodology. The buildings considered – four in total – include conventional and base-isolated versions of both braced frame and moment resisting frame lateral systems. In this paper, the seismic response of

[1]Assistant Professor, Dept. of Civil and Env. Engineering, Utah State University, Logan, UT 84322-4110
[2]Research Engineer, NORSAR, Gunnar Randers vei 15, PO Box 53, NO-2027, Kjeller, Norway
[3]Structural Engineer, Gandhi Consulting Engineers and Architects, New York NY 10038
[4]Graduate Research Assistant, Dept. of Civil and Env. Engineering, Utah State University, Logan, UT 84322-4110

the buildings is analyzed to scenario earthquake events. Results of a follow-up loss estimation study, which uses the statistical response data as input, are reported in a companion paper (Ryan, 2010). The complete loss estimation study considers nine discrete earthquake scenarios representing various annual probabilities of exceedance on the seismic hazard curve, but response measures for only three of the nine scenarios are presented here.

Building Design Assumptions

Hypothetical three-story conventional and base-isolated braced frame and moment resisting frame buildings were designed by Forell/Elsesser Engineers Inc. for use in this study. These office buildings (occupancy category II and importance factor $I = 1.0$) were designed by the *Equivalent Lateral Force Method* based on 2006 International Building Code (ICC, 2006), ASCE 7-05 (ASCE, 2005), and AISC 341-05 (AISC, 2005). The buildings were designed for Los Angeles, CA location (Latitude: 34.50 N, Longitude: 118.2 W) on stiff soil (site class D). The mapped spectral accelerations for this location are $S_s = 2.2g$ for short periods and $S_1 = 0.74g$ for a 1 second period (g = acceleration due to gravity).

The conventional buildings were detailed for high ductility as a special concentric braced frame (SCBF) and a special moment resisting frame (SMRF). The isolated buildings, with lower ductility requirements, were detailed as an ordinary concentric braced frame (OCBF) and an intermediate moment resisting frame (IMRF). The SMRF uses pre-qualified (AISC, 2005) reduced beam section (RBS or "dogbone") connections, while the IMRF uses welded unreinforced flange, welded web (WUF-W) connections. Relative to the SCBF, the OCBF allows for relaxation of brace slenderness ratio and gusset plate detailing requirements. Design force reduction factors for the buildings were: $R = 6$ for the SCBF, $R = 8$ for the SMRF, $R = 1$ for the OCBF and $R = 1.67$ for the IMRF. In addition, design drift limits were taken to be 2.5% for the conventional buildings and 1.5% for the isolated buildings. The design of the braced frames was force controlled while the design of the moment frames was drift controlled.

The basic building configuration is shown in Figure 1, with lateral frames for the different buildings designated in color. The buildings are 55 m by 36.6 m (180 ft by 120 ft) in plan, with story heights of 4.57 m (15 ft) and column spacing of 9.15 m (30 ft) in each direction. The lateral loads of the SCBF are carried by a single braced bay on each side of the building perimeter. The bracing in the OCBF is similar but is fanned outward from the top down to the base to maximize the resistance to local uplift at the isolation level. For both moment frame buildings, lateral resistance is provided by two 5-bay perimeter moment frames in the longitudinal direction, and two 3-bay perimeter and two 2-bay interior moment frames in the transverse direction.

Seismic masses were calculated from anticipated gravity loads on the floors and roof, which in addition to the weight of the structural frame members, includes 3.11 to 3.11 kPa (65 to 67 psf) dead load per floor, and 0.96 kPa (20 psf) for cladding around the building exterior. Table 1 lists the seismic weights of each story for each building.

The design displacement D_D of the isolators in the design earthquake and the maximum displacement D_M in the MCE at the center of rigidity are computed as (ASCE, 2005):

$$D_D = \frac{gS_{D1}T_D}{4\pi^2 B_D} \quad , \qquad D_M = \frac{gS_{M1}T_M}{4\pi^2 B_M} \tag{1}$$

where T_D, T_M are effective isolation periods; B_D, B_M are coefficients that modify the spectrum for damping; and S_{D1}, S_{M1} are the 1 second spectral accelerations for the corresponding events. Target values of T_M and effective damping β_M were chosen for the MCE, while design values T_D and β_D were determined by iteration (Table 2). The total isolator displacement in Table 2 accounts for displacement amplification due to accidental torsion. The isolation devices have not been designed in detail so as to keep the study neutral with respect to isolation system.

Computational Models for Seismic Evaluation

Models for evaluation were developed using the guidelines of ASCE 7 (ASCE 2005) for design of new buildings and ASCE 41 (ASCE 2007) for evaluation of existing buildings. Detailed three dimensional (3D) numerical models of all buildings were developed in the OpenSees computational environment. The mass centers were shifted by 5% of the longest plan dimension in each direction to account for accidental torsion, and rigid diaphragm constraints

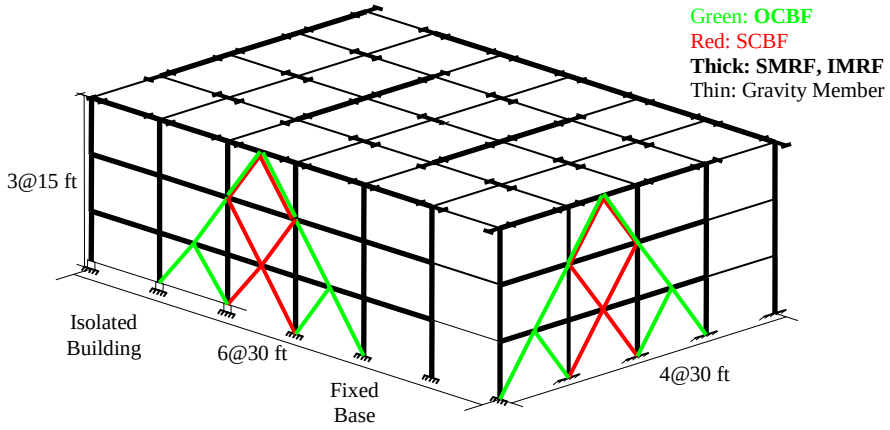

Figure 1. 3D view of the building elevation and plan layout, with SMRF and IMRF lateral frames in black, SCBF frames in red, and OCBF frames in green.

Table 1. Seismic weights of each of the buildings summed by floor

Seismic Weight	Conventional SCBF	Isolated OCBF	Conventional SMRF	Isolated IMRF
Base	-	7574 kN (1702 k)	-	7765 kN (1745 k)
Story 1	7962 kN (1790 k)	7914 kN (1779 k)	8561 kN (1924 k)	8085 kN (1817 k)
Story 2	7957 kN (1789 k)	7871 kN (1768 k)	8532 kN (1918 k)	8063 kN (1812 k)
Roof	8304 kN (1867 k)	8183 kN (1838 k)	8922 kN (2005 k)	8728 kN (1962 k)

Table 2. Design parameters for the isolation systems

Isolator Properties	DBE	MCE
Effective Period	T_D = 2.77 sec	T_M = 3.07 sec
Effective Damping	β_D = 24.2 %	β_M = 15.8 %
Isolator Displacement	D_D = 32.1 cm (12.7 in.)	D_M = 61.7 cm (24.3 in.)
Total Displacement	D_{TD} = 38.8 cm (15.3 in.)	D_{TM} = 74.6 cm (29.4 in.)

were applied at each floor level. All columns and beams of moment resisting and braced bays were modeled using force-based frame hinge elements that combine finite length "plastic hinge" regions at the element ends with an interior elastic region (Scott, 2006). Columns were modeled using *fiber* sections, while beams were modeled using stress resultant section behavior. The steel stress-strain or moment-curvature relations, as applicable, were assumed to be bilinear with 3% strain hardening. Gravity beams were modeled using elastic frame elements with moment releases at both ends. In the conventional buildings, moment resisting and gravity columns were fixed and pinned at the base, respectively; while in the isolated buildings, fixed connections were assumed at all beam-column joints at the base level. Energy dissipation was applied to each structure or superstructure using tangent stiffness proportional damping calibrated to give 2.5% damping at their respective first mode frequencies.

In the moment frame buildings, panel zone flexibility was explicitly modeled using a rotational spring that simulates the shear force/deformation behavior of the panel zone. Also, for the RBS connections in the SMRF building, three frame elements were used to represent beams with tapered flange, wherein plastic hinge element that represents the region between the flange cutouts was sandwiched between elastic end elements. In the braced frame buildings, a single brace was represented by two nonlinear frame elements with 5% initial camber in the out-of-plane direction that causes buckling to initiate (Uriz, 2008). The connection geometry was also modeled using finite length elastic frame elements for gusset plates, which were sufficiently flexible in the out-of-plane direction such that the braces were effectively pinned.

A model was developed for the behavior of isolation devices that incorporates a composite force-deformation relation in each direction that could represent either elastomeric or friction pendulum devices. An elastic column element and an elastic-perfectly plastic spring were assembled in parallel to obtain the composite bilinear lateral force-deformation behavior for a single isolator. The elastic-perfectly plastic spring is a bidirectionally coupled element with a circular yield surface that exhibits identical resistance in any direction in the *x*-*y* plane. The vertical resistance was represented by a nonlinear elastic spring with compressive stiffness calibrated to a vertical frequency of 10 Hz, and a tensile stiffness equal to 1% of the compressive stiffness. The energy dissipation in the isolator model is provided by hysteresis in the lateral directions and viscous damping in the vertical direction.

Fundamental Properties

Eigenvalue analysis was carried out on the various building models to evaluate their elastic dynamic properties. For eigenvalue analysis, the isolators were modeled as linear springs with stiffness corresponding to the design period T_D = 2.77 sec. The fundamental periods of the building are reported as follows: T = 0.5 sec for the SCBF, 3.05 sec for the isolated OCBF, 0.89 sec for the SMRF, and 3.23 sec for the isolated IMRF. The lengthening of the first mode period of the isolated buildings relative to the isolation period is due to both structure flexibility (especially prominent in the IMRF) and the torsional nature of the first mode. The IMRF without isolators has a fundamental period of 1.5 sec.

Nonlinear static analysis (or pushover analysis) was carried out under an inverted triangle load pattern to determine the base shear capacity and post-yield behavior based on the various

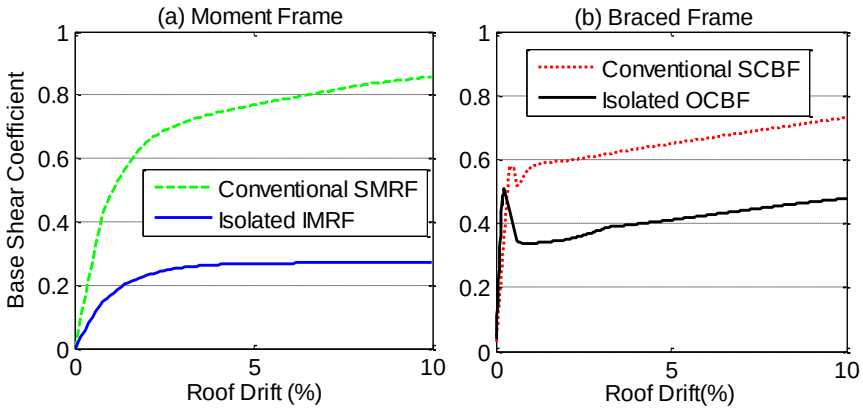

Figure 2. Capacity curves of (a) moment frame buildings and (b) braced frame buildings generated by pushover analysis.

building models. Capacity curves for both the braced frame and moment frame buildings are plotted in Figure 2. The braced frame buildings exhibit a sudden loss of stiffness, presumably associated with a buckling mode, followed by load redistribution and recovery; in contrast the capacity curves of the moment frame buildings are smooth. While the SMRF model hardens out to large deformation limits, the IMRF capacity curve essentially flattens after complete yielding. The isolated OCBF has about 70% of the strength of the SCBF, but the isolated IMRF has less than half the strength of the SMRF.

Ground Motion Selection

The following general procedure was used to select ground motions for loss estimation (ATC, 2007). First, a hazard curve was defined that quantifies ground motion intensity versus frequency of occurrence. Individual points along the hazard curve represent various earthquake scenarios ranging from frequent small events to large rare events. For several distinct earthquake scenarios, target spectra were generated and ground motions were selected and amplitude scaled to best match the target spectra.

USGS national seismic hazard maps (Frankel, 2000) were consulted to generate uniform hazard spectra (target spectra) for nine selected events: which correspond to 10, 40, 72, 200, 475, 975, 1500, 2475, and 5000 year return periods. To modify the target spectra for site effects, spectral site modification factors that depend on both ground motion intensity and period were developed from next generation attenuation (NGA) relations (e.g. Campbell, 2008).

Three suites of ground motion were developed to represent the 72, 475, and 2475 year return period events. Using USGS seismic deaggregation data (Frankel, 2000), ground motions were selected according to the percentage contribution of magnitude and distance pairs to the seismic hazard for a given scenario. For these three scenarios, 20 recorded natural ground motions that conform to the magnitude, distance and site class were selected from the PEER NGA database and amplitude scaled to match the target spectrum. Each bin was also amplitude scaled again to represent the two remaining nearest earthquake scenarios. While using recorded ground motions was considered to be ideal, we replaced some of the recorded motions with frequency modified motions to obtain a better match between the target hazard spectra and the

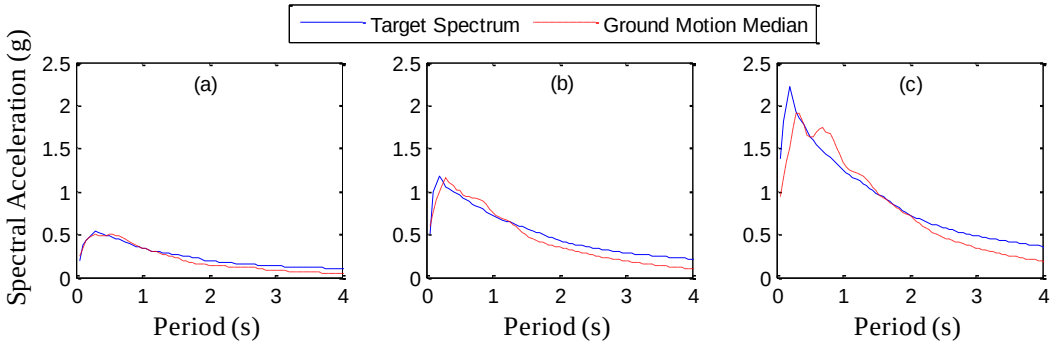

Figure 3. Target and median spectra for (a) 72 year, (b) 475 year, and (c) 2475 year earthquake scenarios.

median response spectra in the long period range. These three ground motions bins are listed on the NEES TIPS project website (NEES TIPS 2009). Figure 3 compares the median response spectra for each suite scaled to the corresponding hazard level.

Comparative Results of Nonlinear Response History Analysis

Nonlinear response history analyses (RHA) were carried out to comparatively evaluate the structural response of each of the four buildings when subjected to the ground motion suites described previously. The statistical distribution of peak story drift, peak floor acceleration, and peak isolator deformation for 72, 475 and 2475 year events are presented. Story drifts were evaluated separately in each direction as the maximum at any of the four corners of the building. Total floor acceleration at the center of mass and isolator deformations (maximum over devices) were evaluated as the vector sums of the demands in the X and Y directions. The median and 84th percentile responses were computed assuming the data to be lognormally distributed.

Response in Frequent (72 Year) and Design (475 Year) Events

Although not explicitly identified in building codes, we interpret the design objectives for the isolated buildings as: 1) to suppress yielding (especially for the OCBF designed for R=1) and 2) to attenuate accelerations to well below the peak ground acceleration (PGA) in the design (475 year) event. Yield story drifts were estimated for each building based on the capacity curves (Fig. 2) and approximate design principles, which are 0.45% for the SCBF, 0.33% for the OCBF, 1.2% for the SMRF, and 1.5% for the IMRF. Accordingly, the isolation system statistically prevents yielding in both the design and frequent events for both braced and moment frame lateral systems, while the conventional counterparts are observed to be statistically likely to yield, especially in the design event (Fig. 4). In these events, isolation is observed to reduce the median story drifts of the OCBF by a factor of 2 to 4 relative to the conventional SCBF [Fig. 4(a)-(b)], but the drift reduction in the IMRF relative to the SMRF is generally 50% or less [Fig. 4(d)-(f)]. Isolation is less effective at reducing drifts in the moment frame due to its relative flexibility. Furthermore, even if the moment frame does not yield, drifts as large as 1.5% are expected to generate some damage in nonstructural components.

Regarding accelerations, the floor accelerations in the conventional buildings are increasingly amplified with height relative to PGA, as expected, while the floor accelerations in

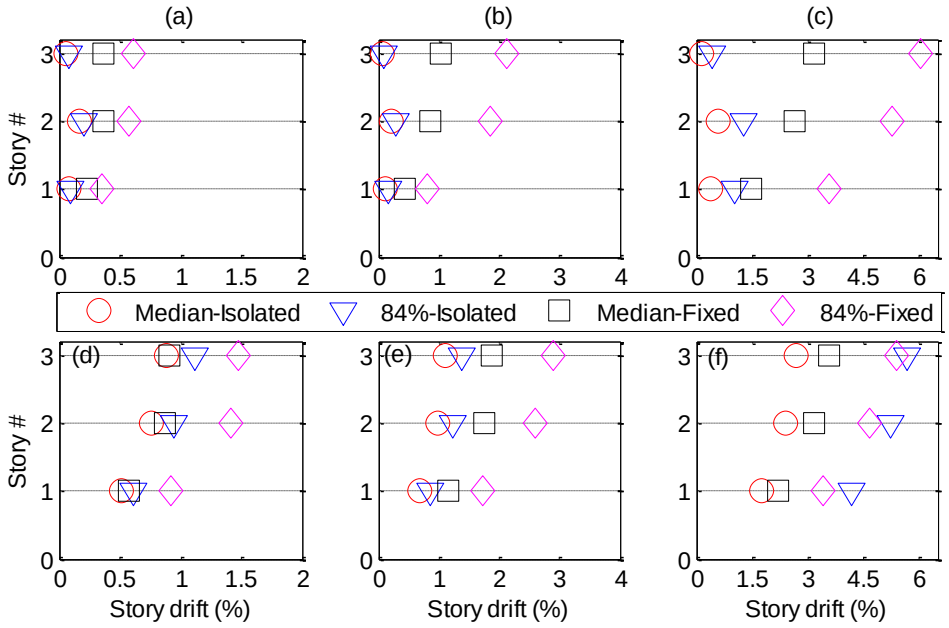

Figure 4. Peak transverse direction story drift ratio demands for: (a)-(c) braced frame buildings in 72, 475 and 2475 year events, respectively; and (d)-(f) moment frame buildings in 72, 475 and 2475 year events, respectively.

the isolated buildings are reduced relative to PGA (Fig. 5). Note that the accelerations at level 0 (ground) designate PGA and the accelerations between 0 and 1 designate accelerations just above the isolators (Fig. 5). For example, in the design event (PGA = 0.61*g*), the median roof acceleration is increased to 1.05 and 1.15*g* in the SCBF and SMRF, respectively, and reduced to 0.22 and 0.3*g* in the OCBF and IMRF, respectively. Based on these results, the design objectives appear to have been met.

For the design and frequent events, the demands in the isolated building can be predicted with high confidence as the dispersions (reflected in the difference between median and 84th percentile responses) in story drifts [Fig. 4(a)-(b) and 4(d)-(e)] and especially total floor accelerations [Fig. 5(a)-(b) and 5(d)-(e)] are quite small. Since the isolated buildings respond elastically their dispersion in story drift is limited relative to the conventional buildings. One possible explanation for the small dispersion in acceleration is that period lengthening generally has a smoothing effect on spectral accelerations, which are correlated to floor accelerations. Another explanation is that isolation leads to increased relative attenuation with increasing PGA, such that the overall dispersion in floor acceleration tightens relative to the dispersion in PGA.

The relative drift reduction is even smaller for the frequent event compared to the design event, wherein median story drift demands are reduced only slightly relative to the conventional buildings [Fig. 4(a), 4(d)]. To interpret, the isolation system becomes less effective for earthquake intensities lower than the design event because it is not fully activated [median deformation = 12.8 cm (5.0 in) for the OCBF and 9.5 cm (3.8 in) for the SCBF (Table 3) relative to the design displacement of 32 cm (12.7 in) (Table 2)], resulting in a higher effective stiffness and a smaller period separation compared to the superstructure. This behavior has greater significance for the more flexible moment frame system; as a result accelerations in the moment

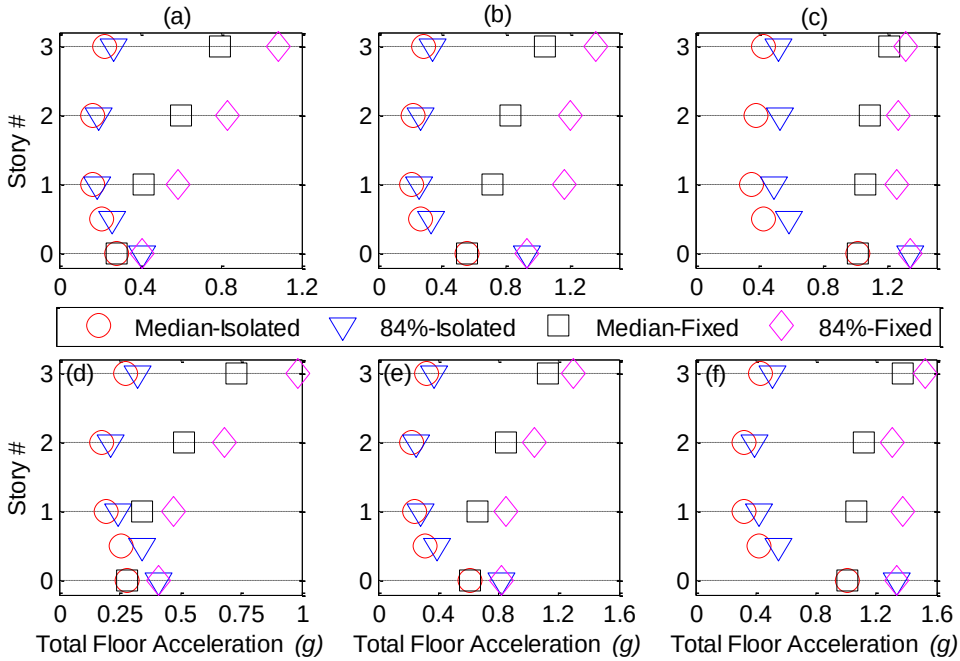

Figure 5. Total floor acceleration demands for (a)-(c) braced frame buildings, and (d)-(f) moment frame buildings, in 72, 475 and 2475 year events, respectively.

Table 3. Peak isolator displacement demands under scenario earthquakes

Scenario	Statistics	Isolator Displacements	
		OCBF	IMRF
72 year	Median	12.80 cm (5.04 in.)	9.53 cm (3.75 in.)
	84%	20.22 cm (7.96 in.)	16.81 cm (6.62 in.)
475 year	Median	33.53 cm (13.20 in.)	30.73 cm (12.1 in.)
	84%	64.14 cm (25.25 in.)	46.58 cm (18.34 in.)
2475 year	Median	89.28 cm (35.15 in.)	61.41 cm (24.18 in.)
	84%	148.34 cm (58.40 in.)	97.99 cm (38.58 in.)

frame are barely attenuated below the PGA in the frequent event [Fig. 5(d)].

Response in MCE (2475 Year Event)

Story drifts for the isolated buildings are generally reduced in the MCE (2475 year event) relative to the conventional buildings, but the same confidence in the superior performance of isolation in a design event cannot be extended to the MCE. For the braced frame buildings, both the median and 84th percentile peak story drift demands (0.6 and 1.25%) of the OCBF are reduced substantially relative to the SCBF (3 and 6%), but the dispersion in story drifts is larger than before [Fig. 4(c)]. However, in the moment frame buildings, the median peak story drift is reduced from about 3.6% for the SMRF to about 2.7% for the IMRF, but the 84th percentile story drift demands are comparable in both [Fig. 4(f)]. The increase in the 84th percentile drift is the result of outliers; for example, two motions induce peak drift demands on the order of 15-16% in the isolated IMRF [Fig. 6(b)]. Similar outliers are not observed for the SMRF, as several

motions induce peak story drifts on the order of 5-8%. One outlier is observed for the OCBF [Fig. 6(a)], but the peak drifts in the OCBF are otherwise so much lower than for the SCBF that this outlier does not have a notable negative effect on the statistics.

Several studies have drawn conclusions that explain why the outliers occur, e.g. yielding is self-limiting in conventional structures but self-propagating in isolated structures (Kikuchi, 2008), and isolated buildings are more sensitive than conventional buildings to statistically reasonable uncertainties in ground motions (Politopoulos, 2005). Furthermore, the observed flattening of the capacity curve of the isolated IMRF beyond the ultimate strength likely amplifies large yield excursions compared to the other buildings that continue to strain harden at large drifts (Fig. 2). Through the simple force balance concept, structural yielding helps to limit acceleration demands. The isolated buildings are observed to be very effective in limiting total floor accelerations to levels well below the PGA [Fig. 5(c) and 5(f)].

The median isolator deformation in the 2475 year event (89 cm for OCBF) (Table 3) exceeds the MCE displacement D_M = 61.7 cm (Table 2), and the 84th percentile deformation of 148 cm (OCBF) and 98 cm (SCBF) (Table 3) exceeds D_{TM} = 74.6 cm (Table 2). Since the seismic gap length and moat wall location are at the designer's discretion, the potential collision with a moat wall was *not* simulated in this study. However, under reasonable design practices, collisions with the outer moat wall would be expected for some of the ground motions considered, and would transmit high frequency waves up through the superstructure. These phenomena, and the potential for collapse in extreme motions, should be investigated further.

Conclusions

The seismic response of isolated and conventional three-story steel braced frame and moment frame buildings was compared for three earthquake scenarios. The isolated buildings met their performance objectives in the design event, and their response can be predicted with high confidence. However, the flexibility of the moment frame induced rather large drifts that could lead to damage in drift sensitive nonstructural components for moderate events. The isolated moment frame was relatively weaker than the other three buildings, which led to extreme drift demands for some of the motions in the 2475 year event, and as a result large

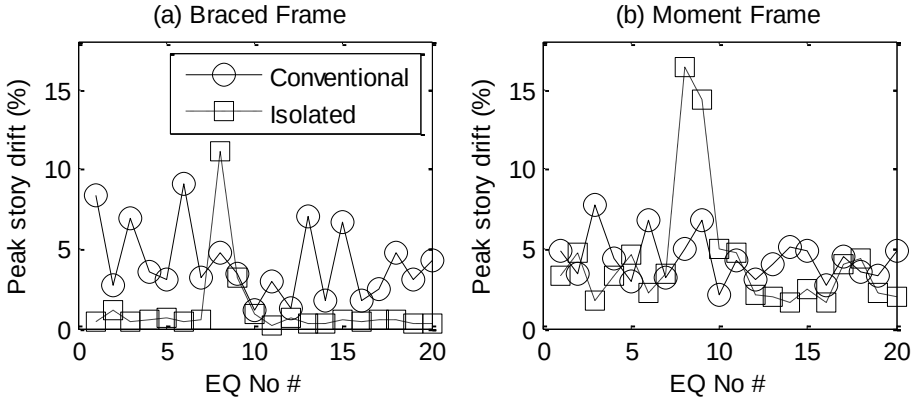

Figure 5. Peak drift in any story sampled over individual ground motions for the 2475 year event; (a) braced frame buildings, and (b) moment frame buildings.

dispersion. Overall, the isolation of the braced frame was more effective than isolation of the moment frame, and it might be worthwhile to stiffen and strengthen the isolated moment frame.

Acknowledgments

This material is based upon work supported by the National Science Foundation under Grant No. CMMI-0724208. Any opinions, findings, and conclusions expressed here are those of the authors and do not necessarily reflect the views of the National Science Foundation.

References

American Institute of Steel Construction (AISC), 2005. *AISC 341-05 Seismic Provisions for Structural Steel Buildings*, Chicago, IL.

American Society of Civil Engineers (ASCE), 2005. *ASCE 7-05 Minimum Design Loads for Buildings and Other Structures*, Reston, VA.

American Society of Civil Engineers (ASCE), 2007. *ASCE 41, Seismic Rehabilitation of Existing Buildings*, Reston, VA.

Applied Technology Council, 2007. *ATC-58: Guidelines for Seismic Performance Assessment of Buildings*, 35% Complete Draft, Washington, DC.

Campbell, K. W. and Bozorgnia, Y., 2008. NGA ground motion model for the geometric mean horizontal component of PGA, PGV, PGD and 5% damped linear elastic response spectra for periods ranging from 0.01 to 10 s, *Earthquake Spectra*, **24**, 139-171, EERI.

Frankel, A. D. et. al., 2000. USGS national seismic hazard maps, *Earthquake Spectra*, **16**, 1-19, EERI.

International Code Council (ICC), 2006. *International Building Code (IBC)*, Falls Church, VA.

Kikuchi, M., Black, C. J., and Aiken, I. D., 2008. On the response of yielding seismically isolated structures, *Earthquake Engineering and Structural Dynamics*, **37**, 659-679.

NEES TIPS: Tools for Isolation and Protective Systems, 2009. http://www.neng.usu.edu/cee/faculty/kryan/NEESTIPS/index.html [13 July 2009].

Politopoulos, I. and Sollogoub, P., 2005. Vulnerability of elastomeric bearing isolated buildings and their equipment, *Journal of Earthquake Engineering*, **9**, 525-545.

Ryan, K. L., Sayani, P. J., Dao, N. D., Abraik, E., and Baez, Y. M., 2010. Comparative life cycle analysis of conventional and base isolated theme buildings, *Proc. 9th U.S. National/10th Canadian Conference on Earthquake Engineering*, Paper No. 1563, Toronto, Canada.

Scott, M., H., and Fenves, G., L., 2006. Plastic hinge integration methods for force-based beam-column elements, *J. Struct. Eng.*, **132**, 244-252, ASCE.

Uriz, P., Filippou, F., C., and Mahin, S., A., 2008. Model for cyclic inelastic buckling of steel braces, *J. Struct. Eng.*, **134**, 619–628, ASCE.